PHYSICAL REVIEW A **83**, 021406(R) (2011)

Redistribution of vibrational population in a molecular ion with nonresonant strong-field laser pulses

W. A. Bryan,[1,2,*] C. R. Calvert,[3] R. B. King,[3] G. R. A. J. Nemeth,[1,2] J. D. Alexander,[3] J. B. Greenwood,[3] C. A. Froud,[2] I. C. E. Turcu,[2] E. Springate,[2] W. R. Newell,[4] and I. D. Williams[3]

[1]*Department of Physics, Swansea University, Singleton Park, Swansea SA2 8PP, United Kingdom*

[2]*STFC Rutherford Appleton Laboratory, Harwell Science and Innovation Campus, Didcot OX11 0QX, United Kingdom*

[3]*School of Mathematics and Physics, Queen's University Belfast, Belfast BT7 1NN, United Kingdom*

[4]*Department of Physics and Astronomy, University College London, London WC1E 6BT, United Kingdom*

(Received 3 November 2010; published 28 February 2011)

We present an experimental demonstration of nonresonant manipulation of vibrational states in a molecule by an intense ultrashort laser pulse. A vibrational wave packet is generated in D_2^+ through tunnel ionization of D_2 by a few-cycle pump pulse. A similar control pulse is applied as the wave packet begins to dephase so that the dynamic Stark effect distorts the electronic environment of the nuclei, transferring vibrational population. The time evolution of the modified wave packet is probed via the D_2^+ photodissociation yield that results from the application of an intense probe pulse. Comparing the measured yield with a quasiclassical trajectory model allows us to determine the redistribution of vibrational population caused by the control pulse.

DOI: 10.1103/PhysRevA.83.021406 PACS number(s): 33.80.Gj, 33.20.Xx, 42.50.Hz, 82.53.Eb

Advances in ultrafast laser technology now allow the motion of vibrational wave packets to be imaged through the use of nonresonant strong-field laser pulses [1–4], with the experiments generally carried out on single-electron molecular ions or electronically isolated systems. In particular the hydrogen diatomics provide a crucial testbed, leading to new discoveries in molecular dynamics and control [5]. In recent years, several substantial developments have been made in this field, owing to the production of few-cycle near-infrared (NIR) laser pulses with durations on subvibrational time scales. Such pulses are ideal for nonresonant manipulation of potential landscapes for steering molecular wave-packet evolution. In recent pioneering studies, the ability to control electron localization during molecular dissociation has been demonstrated in the deuterium molecular ion [6–9]. Here, the electric field of the laser pulse has been used to couple the electronic states in the molecular ion and guide the electron during the photodissociation (PD) event. Innovative imaging techniques have also been developed through studies in this molecule, where the "molecular clock" [10] and probing attosecond dynamics by chirp encoded recollision (PACER) [11] schemes have availed of electron-recollision dynamics [12]. In addition, XUV attosecond pump pulses have been employed [13] to initiate vibrational dynamics, with the authors reporting the necessity to consider the influence of the NIR probe. The evolution of nuclear wave packets in the molecular ion underpin each of these developments, and the ability to manipulate such vibrational dynamics promises to provide a significant step in enhancing molecular control schemes [14]. However, while there has been progress in time-resolved imaging (see [5] and references therein), experimental control of the vibrational distribution, which dictates wave-packet evolution, has remained elusive.

Here, we apply a three-pulse sequence to create, manipulate, and probe a vibrational wave packet and report vibrational redistribution in a bound wave packet in D_2^+. Through probing the modified wave packet, we find systematic trends observed in the experimental results that can be predicted by quasiclassical simulations and hence recover the redistributed vibrational-state populations. While other multipulse studies have demonstrated selective dissociation of a vibrational wave packet [15,16], this current work constitutes a significant breakthrough, as the ability to modify the bound vibrational superposition provides a platform for future studies of molecular control (e.g., [14]).

The scheme for wave-packet control is sketched in Fig. 1. The pump pulse initiates tunnel ionization of D_2, populating a coherent superposition of vibrational states in the electronic ground state ($1s\sigma_g$) of the D_2^+ molecular ion. The manipulation pulse is applied after some delay, during which the vibrational wave packet has evolved in time [see Figs. 1(b) and 1(c)], and acts to modify the bound wave packet. Finally, the subsequent evolution of the modified wave packet is mapped by a probe pulse via PD of the molecular ion.

The D_2^+ wave packet created in this scheme is in a broad range of vibrational states, each evolving at a different frequency. The wave packet initially oscillates across the bound potential surface in a localized form. However, due to the anharmonicity of the potential, it rapidly undergoes quantum dephasing [shown in Figs. 1(b) and 1(c)] so that the wave packet becomes delocalized across the full extent of the potential [2,4,17]. The spatial and temporal profile of the vibrational wave packet is thus inherently dictated by the vibrational-population distribution.

While the vibrational distribution is initially set by the pump process, theoretical predictions suggest that the wave packet can be actually manipulated by an ultrashort laser pulse, leading to modified vibrational-state distributions [18,19] via mechanisms described in [20,21]. It has been noted that some of the most significant redistribution effects occur when the modification pulse is timed to coincide with the initial dephasing of the wave packet [19,22]. The experimental approach to this study therefore required three intense laser pulses with variable and interferometrically stable delays. A commercial 30-fs Ti:sapphire laser, with a central wavelength

*w.a.bryan@swansea.ac.uk

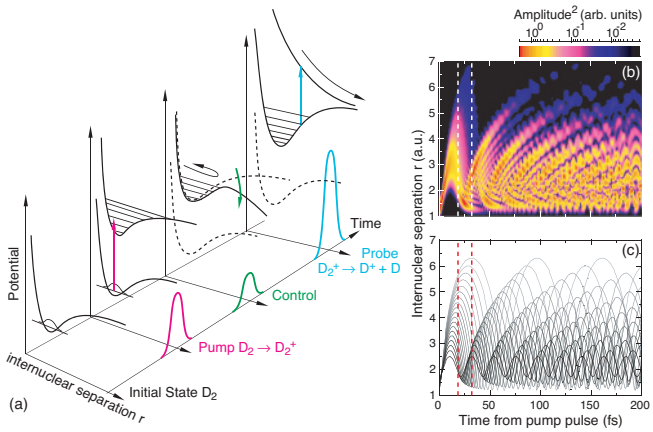

FIG. 1. (Color online) Schematic of the pump-modify-probe scheme and unperturbed vibrational wave-packet motion. (a) The pump pulse ($I_{pump} = 0.4$–1.1×10^{14} Wcm^{-2}) ionizes $D_2 \rightarrow D_2^+$ creating a vibrational wave packet. Following a delay of tens of femtoseconds, the modifying pulse ($I_{mod} = 1.3$–3.7×10^{13} Wcm^{-2}) distorts the molecular potential-energy surface, causing the wave packet to rapidly adjust. The population redistribution is imaged by photodissociating the $D_2^+ \rightarrow D^+ + D$ in the probe pulse ($I_{probe} = 0.6$–2×10^{14} Wcm^{-2}). The quoted ranges indicate the active intensities caused by the overlap of the focal volume with the instrument aperture. (b) and (c) The unperturbed vibrational wave packet. The solutions to the time-dependent Schrodinger equation (b) and current quasiclassical model (c) are compared. The region over which the manipulation pulse is applied is indicated by vertical dashed lines.

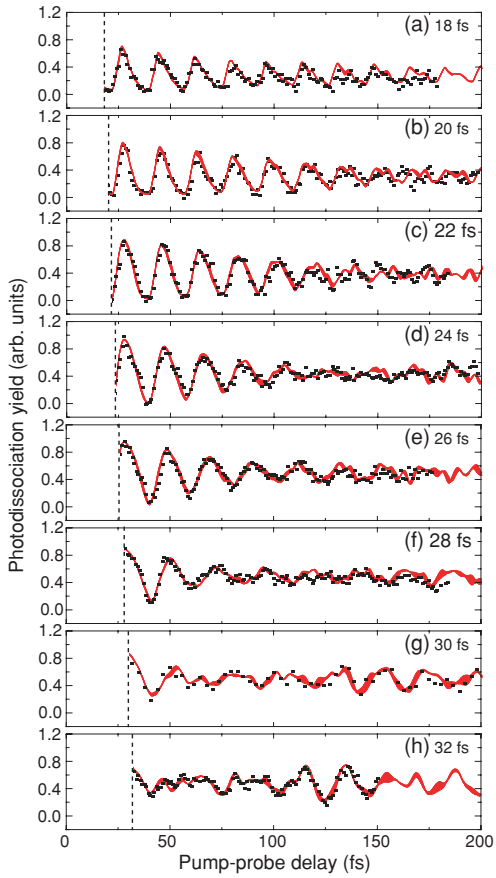

FIG. 2. (Color online) Experimental PD yield (black dots) for pump-modification-pulse delay times from (a) 18 fs to (h) 32 fs. The corresponding focal-volume-integrated yield is given by the solid (red) line and the varying vertical thickness indicates the uncertainty in fitting the experimental results.

of 790 nm and bandwidth of 35 nm, generated 1 mJ pulses at 1 kHz, which were further broadened to 140 nm by self-phase modulation in an argon-filled hollow fiber with a pressure gradient [23]. Following compression by a series of chirped mirrors, the 240-μJ, 10-fs pulse was split into three pulses with independent delays in a nested Mach-Zehnder interferometer, resulting in 32 μJ pump, 11 μJ manipulation, and 35 μJ probe pulses. The synchronization of the three pulses was established using a second-harmonic autocorrelator containing a 10-μm BBO crystal. The three pulses were combined collinearly and reflection focused into an effusive jet of room temperature D_2 in the interaction region of an ion time-of-flight mass spectrometer used to energetically resolve D^+ products as a function of delays. The spectrometer contained a 250-μm aperture, hence only the fragmentation of molecules aligned to within a few degrees of the probe-polarization direction was observed, essentially reducing this to a one-dimensional problem.

Figures 2(a)–2(h) display the experimental PD yield as a function of probe delay for a sequence of discrete manipulation-pulse delays ranging from 18 to 32 fs. We have isolated the contribution of the vibrational wave packet to the PD yield as discussed in [4]; a bandpass ($25 < f < 400$ THz) filter is applied, whereby the high-frequency cutoff smooths subcycle noise and the low-frequency cutoff removes the effects of rotational wave packets in the neutral molecule [24]. Each set of data describes the behavior of the modified wave packet resulting from the effect of the control pulse. As the PD probing event is enhanced near the outer turning point of the $1s\sigma_g$ potential well, oscillations in the yield serve to map the wave-packet motion [25]. For instance, in Fig. 2(a), with the control pulse at 18 fs, it can be deduced that the modified wave packet evolves in a form that remains well localized as it propagates beyond 150 fs. Since the wave packet is oscillating across the potential, this results in a periodic PD yield with strong signal when the wave packet is at the outer turning point and weak signal when it is at the inner turning point. On the other hand, in Fig. 2(h), it can be observed that delocalization of the wave packet is an immediate consequence of the application of the manipulation pulse at 32 fs, but with a strong fractional revival seen to occur centered around 125 fs. Figures 2(b)–2(g) demonstrate a systematic trend between these two extremes. Thus it is immediately apparent that coherent wave-packet motion has been manipulated in this study, with each delay enforcing a different outcome on the subsequent wave-packet evolution.

In order to gain a better understanding of this behavior, and to characterize the vibrational-state redistribution, it is instructive to model the influence of the manipulation pulse. In previous studies, we [21] and others [19,20] have carried out full quantum simulations of such control interactions, taking advantage of the fundamental, effective two-state nature of the D_2^+ system. However, to compare with

the experimental results described here, it is necessary to integrate the simulation over the intensity distribution throughout the effective interaction focal volume at each delay. Thus quantum simulations are computationally prohibitive, and instead we have employed a quasiclassical model, which has been shown to be consistent with a Schrödinger-equation approach in D_2^+ [19] and described in detail elsewhere [22].

First, the action of the pump pulse on the D_2 molecule is simulated by extending the nonadiabatic ionization model of Yudin and Ivanov [26] to a molecular system, allowing the vibrational-state population in the $1s\sigma_g$ state of D_2^+ to be evaluated. Second, a noninteracting classical ensemble is created, with weighted quantized vibrational levels to reflect the initial state of the molecule. The wave-packet evolution can thus be approximated by allowing this classical ensemble to propagate on the internuclear potential-energy surface.

Third, the application of the time-delayed manipulation pulse to the propagating ensemble is described by a time-dependent deformation of the potential-energy surface by virtue of the large, dynamic ac Stark shift [20,27]. The resulting deformation of the potential accelerates or decelerates components of the ensemble, depending on their direction of motion, transferring energy into or out of the system. This classical transfer of energy is directly analogous to an impulsive Raman process due to coupling between the ground $1s\sigma_g$ and repulsive $2p\sigma_u$ states. The effect of this energy transfer is to change the relative phase of the ensemble components with respect to the unperturbed system and to transfer population between the vibrational states.

Fourth, the PD yield as a function of probe-pulse delay is obtained from the fraction of the ensemble residing beyond a critical internuclear separation value. This critical-R cutoff approach has previously been shown to be an excellent approximation in full quantum simulations in the same system [25], and was applied here again for computational expediency. Finally, the effect of focal-volume averaging was incorporated in the modeling, with the redistribution process simulated for a broad range of intensities within the focal volume.

The PD yields calculated by integrating the quasiclassical model over the range of intensities measured in the experiment for manipulation-pulse delays in the range 16–34 fs are displayed in Fig. 3. The evolution from a well-localized wave packet displaying periodic signal at short control delay times to

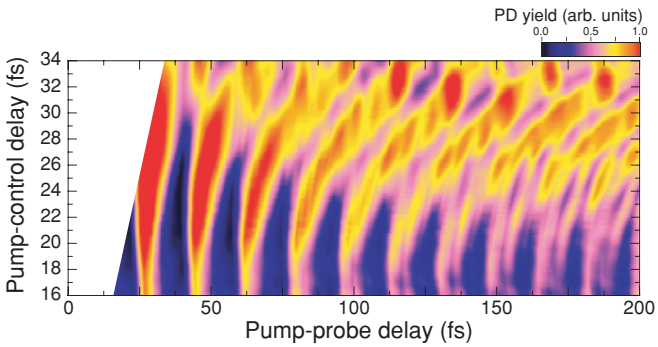

FIG. 3. (Color online) Predicted PD yield integrated over the focal volume for different pump-manipulation-pulse delays between 16 and 34 fs, as a function of pump-probe delay.

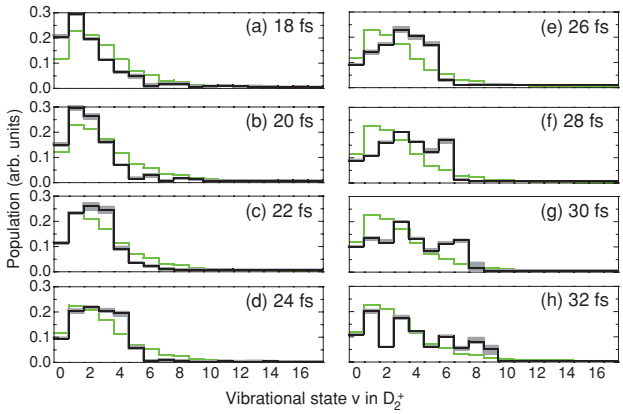

FIG. 4. (Color online) Simulated vibrational distribution for each manipulation-pulse delay. In each plot, the initial distribution created by the pump pulse is given by the light (green) line and modified distribution is given by the dark (black) line. The uncertainty in population (gray bars) is derived from the uncertainty when fitting the experimental PD yield (Fig. 2).

the more dispersed behavior as control-pulse delay is increased is clearly evident. So too are the "islands" in the Fig. 3 color map in the 100–150-fs range observed at longer control delay times, indicative of partial wave-packet revival.

The results of the simulations have also been displayed as a solid line in Fig. 2, where a fitting procedure has been adopted, with pulse intensities varied in order to obtain a best fit. Sources of uncertainty are defining the zero delay time (estimated as 300 as from a linear delay calibration) and the range of active intensities (estimated as better than 8×10^{12} Wcm^{-2} for all three pulses). The agreement in trend with the experimental data (Fig. 2) is strong, indicating that the effect of a manipulation pulse on a bound wave packet in a practical system can be predictable, even in circumstances where experimental volume effects may be expected to blur the outcome.

Most interesting is that the model also returns corresponding predictions for the redistribution of vibrational-state populations. We can thus, through comparison with the experimental PD yield, deduce the modification of the vibrational distribution by the manipulation pulse. These results are shown as dark (black) lines in Fig. 4 for the range of control-pulse delays employed in the experiment. Also shown as a light (green) line in each case is the initial vibrational distribution as predicted by the ionization model. It should be noted that this is not a typical Franck-Condon distribution, but is instead skewed to lower vibrational states, consistent with other studies of ultrashort pulse ionization in D_2 [28,29].

With a delay around 30 fs between the pump and manipulation pulse, the vibrational population is broadly distributed with meaningful population occurring in up to 10 states. The net effect of this operation is that population from lower states is distributed toward higher vibrational levels. By this time, the initial wave packet has already executed a full field-free oscillation and is again moving outwards in R, toward the outer turning point of the potential well. As the potential surface begins to oscillate, it acts to accelerate the wave packet with

the net effect of the dynamic Stark interaction imposing a force acting outwards in R [20,22]. Thus the population is redistributed with portions moving toward large R values, i.e., into higher vibrational states.

The converse occurs if the wave packet is moving inwards in R when the manipulation pulse is applied. Here the outward force is opposing the motion, decelerating the wave packet such that the population is redistributed to a subset of lower vibrational levels. This effect is observed for the shorter control delays in Figs. 4(a)–4(c), leading to the dominance of fewer states and resulting in the oscillatory wave-packet motion of Figs. 2(a)–2(c), where, with fewer states occupied, the wave packet executes localized motion for a longer period of time prior to any dephasing effects.

In this Rapid Communication, we have demonstrated that the modification of a bound vibrational wave packet in D_2^+ by an ultrashort control pulse can be experimentally implemented and quantified. The redistribution of vibrational population can be recovered using a model that incorporates tunnel ionization and dynamic Stark-shift deformation of the potential surface integrated over the focal volume. While this model is approximate, it demonstrates the validity of applying a strong-field treatment to a simple system. In the future, multiple active electronic orbitals and more than two nuclei will add complexity, but may well be theoretically tractable following the reduction to the most significant nuclear coordinates. Calculating polyatomic potential-energy surfaces and polarizabilities is well within the capabilities of modern *ab initio* quantum chemistry software, hence predictions for triatomics such as Carbonyl Sulphide (OCS) are feasible and could be benchmarked against time-dependent density-functional theory [30]. Coherent control [31,32] of complex polyatomic molecules has been demonstrated in the weak ($<10^{10}$ Wcm^{-2}) and intermediate (10^{10} Wcm^{-2} $< I <$ 10^{12} Wcm^{-2}) field regimes; see recent reviews [33,34] for discussions of quantum chemistry, molecular dynamics, wave-packet propagation, and optical control of polyatomic systems.

This work was supported by the Engineering and Physical Sciences Research Council (EPSRC) and the Science and Technology Facilities Council (STFC), United Kingdom. C.R.C. and R.B.K. acknowledge financial support from the Department of Education and Learning (NI). G.R.A.J.N. acknowledges financial support from EPSRC and STFC.

[1] H. Niikura, P. B. Corkum, and D. M. Villeneuve, Phys. Rev. Lett. **90**, 203601 (2003).
[2] Th. Ergler *et al.*, Phys. Rev. Lett. **97**, 193001 (2006).
[3] B Feuerstein *et al.*, Phys. Rev. Lett. **99**, 153002 (2007).
[4] W. A. Bryan *et al.*, Phys. Rev. A **76**, 053402 (2007).
[5] C. R. Calvert, W. A. Bryan, W. R. Newell, and I. D. Williams, Phys. Rep. **491**, 1 (2010).
[6] M. F. Kling *et al.*, Science **312**, 246 (2006).
[7] M. Kremer *et al.*, Phys. Rev. Lett. **103**, 213003 (2009).
[8] G. Sansone *et al.*, Nature (London) **465**, 763 (2010).
[9] B. Fischer *et al.*, Phys. Rev. Lett. **105**, 223001 (2010).
[10] H. Niikura *et al.*, Nature (London) **417**, 917 (2002).
[11] S. Baker *et al.*, Science **312**, 424 (2006).
[12] P. B. Corkum, Phys. Rev. Lett. **71**, 1994 (1993).
[13] F. Kelkensberg *et al.*, Phys. Rev. Lett. **103**, 123005 (2009).
[14] C. R. Calvert *et al.*, J. Phys. B **43**, 011001 (2010).
[15] H. Niikura, D. M. Villeneuve, and P. B. Corkum, Phys. Rev. A **73**, 021402 (2006).
[16] D. S. Murphy *et al.*, J. Phys. B **40**, S359 (2007).
[17] B. Feuerstein and U. Thumm, Phys. Rev. A **67**, 043405 (2003).
[18] D. S. Murphy *et al.*, New J. Phys. **9**, 260 (2007).
[19] T. Niederhausen and U. Thumm, Phys. Rev. A **77**, 013407 (2008).
[20] H. Niikura, D. M. Villeneuve, and P. B. Corkum, Phys. Rev. Lett. **92**, 133002 (2004).
[21] C. R. Calvert *et al.*, J. Phys. B **41**, 205504 (2008).
[22] W. A. Bryan *et al.*, New J. Phys. **12**, 073019 (2010).
[23] J. S. Robinson *et al.*, Appl. Phys. B **85**, 525 (2006).
[24] W. A. Bryan *et al.*, Phys. Rev. A **76**, 023414 (2007).
[25] C. R. Calvert *et al.*, J. Mod. Opt. **56**, 1060 (2009).
[26] G. L. Yudin and M. Yu. Ivanov, Phys. Rev. A **64**, 013409 (2001).
[27] B. J. Sussman, D. Townsend, M. Yu Ivanov, and A. Stolow, Science **314**, 278 (2006).
[28] X. Urbain *et al.*, Phys. Rev. Lett. **92**, 163004 (2004).
[29] A. Saenz, J. Phys. B **33**, 4365 (2000).
[30] K. Burke, J. Werschnik, and E. K. U. Gross, J. Chem. Phys. **123**, 062206 (2005).
[31] S. A. Rice and M. Zhao, *Optical Control of Molecular Dynamics* (Wiley Interscience, New York, 2000).
[32] M. Shapiro and P. Brumer, *Principles of the Quantum Control of Molecular Processes* (Wiley, New York, 2003).
[33] M. Wollenhaupt, V. Engel, and T. Baumert, Annu. Rev. Phys. Chem. **56**, 25(2005).
[34] V. Bonacic-Koutecky and R Mitric, Chem. Rev. **105**, 11 (2005).